Soot size measurement in a swirl stratified premixed ethylene-air flame by a sampling probe and an optical technique

Aurélien Perrier[1,2], Maxime Bouvier[1], Marcos Caceres[1],
Alain Cayre[2], Jérôme Yon[1], Gilles Cabot[1], Frédéric Grisch[1*]
1: Normandie Univ., UNIROUEN, INSA Rouen, CNRS, CORIA, 76000 Rouen, France
2: Safran Aircraft Engines Villaroche, 77550 Moissy-Cramayel, France
* Correspondent author: frederic.grisch@coria.fr

Keywords: Soot size measurement, soot sampling elastic light scattering, turbulent flame

ABSTRACT

An experimental study was performed to measure the size and number density distributions of soot particles produced in a turbulent, stratified (high spatial equivalence ratio gradient), swirled (rotating flow) premixed ethylene-air flame at atmospheric pressure. Soot particle size and number density measurements are initially performed using a Scanning Mobility Particle Sizer (SMPS) combined with a hot gas sampling system. In a second step, the ex-situ measurements were replaced by single-shot measurements recorded with the planar multi-angle light scattering (2D-MALS) laser diagnostic, which is based on the analysis of the scattering angular dependence of the laser light scattered by soot. In order to obtain a well-defined similarity between the measured scalar parameters, the initial data recorded by each measurement technique must be post-processed. For this purpose, the median electric mobility diameters measured by SMPS are converted into diameters of gyration while a time average data processing is applied to the soot size distributions recorded by 2D-MALS. Results obtained in stratified swirled premixed flames by SMPS exhibit an overall good agreement with the optical measurements. Finally, this study demonstrates that 2D-MALS and SMPS are promising in-situ and ex-situ particle sizing techniques that are capable of detecting soot distributions in size and number density in unsteady combustion processes.

1. Introduction

Soot emission is widely recognized as a main issue for its harmful effects on human health and climate. A recent study has shown that soot emissions are the second highest anthropogenic contributor to radiative forcing behind CO_2 (ICAO, 2016), and then play a key role on global warming. A non-negligible part of global soot emission originates from exhaust gases of aircraft engines. Thus, aeronautical emissions are subject to more stringent regulations, among others, on greenhouse gases (i.e. CO2), and pollutants such as nitrogen oxides (NOx) and particulate matter. To achieve an environmental sustainability in aviation, aircraft engine manufacturers need to

develop innovative engine architectures that can significantly reduce particulate and gas emissions. For soot particles, their estimation in terms of size and number density in flames are mainly performed by ex-situ measurement techniques, where soot particles are collected with a sampling probe and then analyzed by an external analysis device. However, ex-situ techniques are often faced with challenging constraints. The presence of an intrusive object inside the combustion chamber such as the sampling probe, as well as the topology of the aerosol along the sampling line, can lead to biased measurements and thus pose a serious representativeness problem. To circumvent this constraint, non-intrusive diagnostics such as optical diagnostics can be implemented to characterize combustion devices without disturbing the combustion process. For example, elastic laser light scattered by soot particles can also provide useful data on the local soot size distribution. The current study presents the results of soot size and number density measurements recorded in stratified swirled premixed flames using two measurement diagnostics, an ex-situ sampling technique coupled with a dilution system and a Scanning Mobility Particle Sizer (SMPS) system and the planar multi-angle light scattering (2D-MALS) laser diagnostic. The following section describes the features of the burner apparatus. The sampling probe method as well as its implementation inside the flame is then outlined. The next section is devoted to the presentation of the principle of the planar multi-angle light scattering diagnostic as well as the description of the associated experimental device. Finally, a comparison between the results issued from both diagnostics is discussed. In this context, we will especially address the issue of distributions in both size and number density. For this particular purpose, a specific methodology has been developed to convert the median electric mobility diameters measured by the SMPS device into gyration diameters while a time average data processing was applied to the soot size distributions measured with the laser diagnostic.

2. SIRIUS burner

The combustion facility selected for the current study is the SIRIUS burner (*SwIrl stRatIfied bUrner for the study of Soot production*) from the French CORIA laboratory (*COmplexe de Recherche Interprofessionnel en Aérothermochimie*). The SIRIUS burner was designed within the framework of the European program SOPRANO (*SOot Processes and Radiation in Aeronautical INOvative combustors*), which included academic research laboratories and aeronautical industrial partners. This facility is intended to obtain a better understanding on the mechanisms governing soot formation in flames in order to get a better control of their formation in aeronautical propulsion systems. The range of flames produced by the SIRIUS burner is wide, from swirling flames to axial flames, from stratified to unstratified flames, and from soot to clean flames. As shown in Fig. 1, the burner exit consists of three concentric tubes with a ceramic cap placed above the inner tube,

forming inner (rich) as well as outer (lean) premixed flow injections. The role of the ceramic cap is devoted to create a bluff body to help to the stabilization of the flame (Fig. 1a). This specific geometry replicates a standard aeronautical injection system, composed of a single pilot injector located on the combustor axis, which is used to stabilize the flame, and a multipoint fuel injection located at larger radial distances. The inner flow is purely axial and the outer flow is swirled thanks to a radial flow injection at the base of the burner (Fig. 1b). The swirl number of the flame is characterized by the Swirl Flow Ratio (SFR), defined as the ratio between the axial and tangential outer flow rates (Fig. 1b):

$$SFR = \frac{\dot{m}_{o,\mathrm{radial}}}{\dot{m}_{\mathrm{o,radial}} + \dot{m}_{o,axial}} \quad (1)$$

The flame stratification is defined by the ratio between Φ_i and Φ_o, corresponding to the equivalence ratios of the inner and outer flows respectively:

$$SR = \frac{\Phi_i}{\Phi_o} \quad (2)$$

Finally, a shielding inert gas coflow is injected through a porous medium which surrounds the external pipe. Inner ($\dot{m}_{\mathrm{int}}$) and outer ($\dot{m}_{\mathrm{o,radial}}$, $\dot{m}_{o,axial}$) flows are controlled thanks to independent mass flowmeters. The current study is performed at atmospheric pressure on three operating conditions (OP) called P1, P2 and P3. Parameters of those OP are detailed in Table 1. They all present the same stratification ratio, i.e. an inner equivalence ratio Φ_{i} of 2.21, and an outer one of 0.74. Only varies SFR to 0.2, 0.25 and 0.3 respectively.

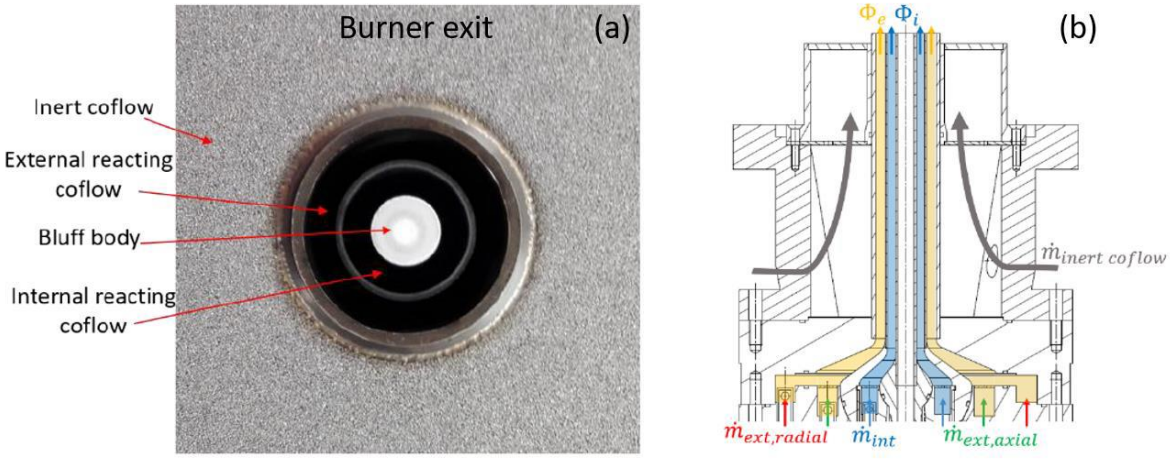

Fig. 1 Presentation of the SIRIUS burner. Top-view of the burner exit (a). Profile-view of the SIRIUS burner

Operation point	Φ_i	Φ_e	Φ_i/Φ_e	SFR
P1	2.21	0.74	3	0.20
P2	2.21	0.74	3	0.25
P3	2.21	0.74	3	0.30

Table 1. Operation points

2. Soot size measurements by a sampling and SMPS analysis

2.1 Soot sampling apparatus for ex-situ measurements

The exhaust gases are sampled by a two-stage dilution device that is similar to the system already detailed in the literature (Mulla, Yon, Lefèvre, Lecordier, & Honoré, 2017). The first dilution stage consists in a 6 mm inox pipe with a 1 mm hole oriented downwards, through which burnt gas produced by the flame enters inside the sampling probe. Nitrogen flow is also injected inside the sampling probe to thermally and chemically quench the intake aerosol flow (i.e. combination of hot gases and soot particles). A vacuum pump is used to produce a negative pressure and hence force the gas suction into the sampling probe. The vacuum pressure is monitored thanks to a differential pressure sensor and maintained constant during the experiments. The second dilution stage is a commercial air diluter Dekati® FPS-4000. The aerosol jet is then transported downstream to a Scanning Mobility Particle Sizer (SMPS) for measuring the soot size and number density distribution. The whole sampling probe is fixed on a translation system to scan the studied flame over a large section i.e. at a Height Above Burner (HAB) ranging between 25 and 75 mm, and at a radial distance from the burner axis from 0 to 40 mm.

One of the main difficulties when using a probe sampling diagnostic to characterize soot aggregates is to ensure that the aerosol that is aspirated and analyzed by the SMPS remains representative of the environment being studied. If no precautions are taken, the size distribution of soot aggregates can be biased due to a multitude of physico-chemical phenomena (Kulkarni, Baron, & Willelke, 2011). This includes, for example, the particle trapping by impaction generated by probe bends and cross-sectional reductions (diaphragms) and/or by diffusion losses. Furthermore, as soot particles tend to easily aggregate along the sampling line, a reduction of the length of the sampling line as well as the number density of the aerosol by diluting it highly are required. Concerning the specific case of soot collection in flames, soot aggregates should also be quenched by dilution for quenching post-sampling chemical reactions.

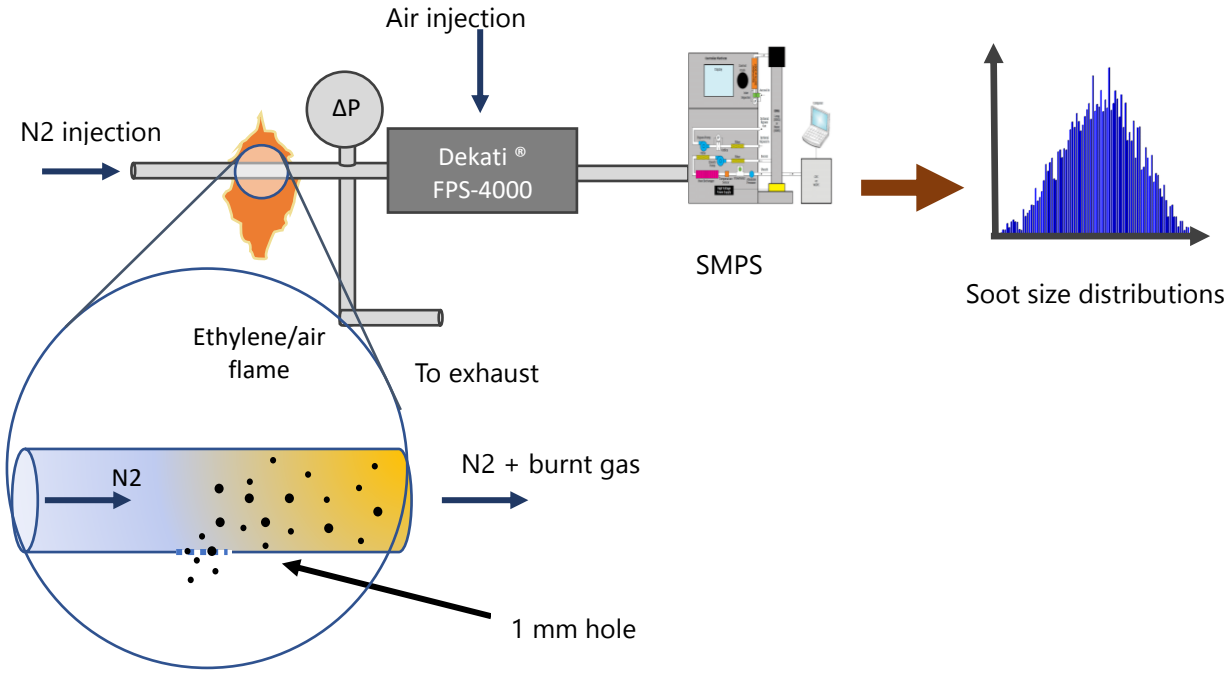

Fig 2. Experimental sampling system

In the current study, the geometry of the sampling probe is simplified thanks to the use of a straight pipe. The sample flow enters the sampling probe through a side port while the cold nitrogen dilution flow enters one of the probe tip orifices. The sample flow immediately diluted by the nitrogen flow is then transported in the commercial air diluter which is an ejector-type diluter, an architecture recognized for its ability to obtain high dilution factors (Giechaskiel, Carriero, Martini, Krasenbrink, & Scheder, 2009) and to avoid particle aggregation. Therefore, the design of the sampling probe was carried out for avoiding any impact on the aerosol size distribution. A preliminary test was performed to calibrate the minimal dilution flow required to obtain satisfying signal-to-noise ratio for the SMPS analysis. The SIRIUS burner is set to P1, the condition for which the production of the soot particles is maximal. The soot sampling probe is positioned at a HAB of 25 mm, along the flame axis ($r = 0\ mm$). This location has been previously identified as one of the locations in which soot particles number density is maximum. The Dekati® FPS dilution factor is fixed to a value near 100, and the vacuum pressure is maintained to 9 mbar. In this configuration, the nitrogen flow rate injected inside the sampling probe was gradually increased by 1 lpm from 3 to 9 lpm. For each flow rate, SMPS measurements were performed and all soot size distributions are reported in Fig. 3. As the flow rate increases, the PDF soot size distributions shift toward smaller diameters, suggesting that particle aggregation is well reduced thanks to the increase of the dilution factor. The measured soot size distributions then converge until a distribution with a peak value close to 20 nm for an injected nitrogen flow rate above 5 lpm. As a consequence, the injected

nitrogen flow rate during the experiments was set to 9 lpm, value exceeding the last value to avoid any particle aggregation along the sampling line and to keep a safety margin in the case in which larger concentrated aerosols could be detected in specific flame locations.

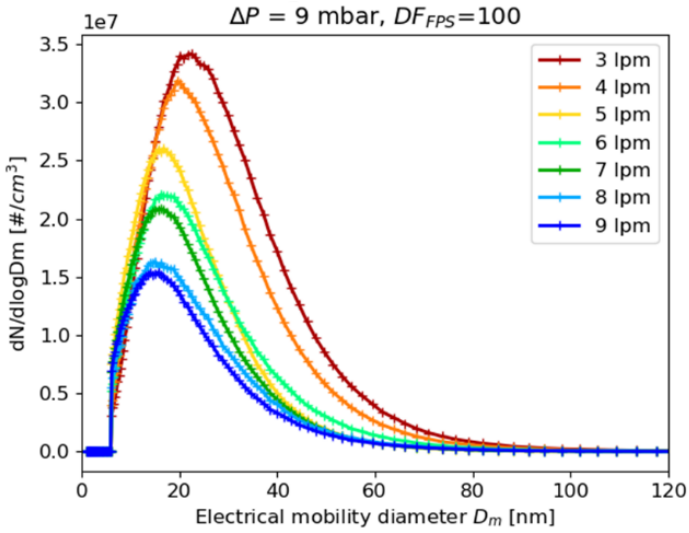

Fig 3. Raw soot aggregate size distribution without dilution (HAB = 25 mm, r = 0 mm) for ΔP=9 mbar at the Dekati® FPS-4000 inlet and a dilution factor set to 100.

2.2 SMPS measurements: Results

The aggregate populations sampled in each flame location display a log-normal type distribution. Using a fitting algorithm, the fitting parameters of their associated log-normal law, i.e. $D_{m,geo}$ the median diameter value, and N_{agg} the number density (number of particles/cm^3) were determined to build their spatial distributions. Results are displayed in Fig. 4. In each image, the left-hand side shows the time-averaged visible flame emission, while the right-hand side shows the median diameter (or the number density) distributions. Overall, it is observed that the soot particles detected in the P_1 condition are the largest in size and in larger quantities compared to P_2 and P_3 conditions. For these three operating conditions, the spatial distributions of the aggregate number density are well correlated to the yellow soot emission. Their location area tends to move off the burner axis when increasing SFR. Considering now the spatial distributions of the median mobility diameters, it can be observed that the largest particles are now located along the burner axis. The lack of a clear correlation between the measured median diameters and the number density simply results of the nature of the soot particles sampled in these two characteristic zones as already demonstrated by results obtained in a previous study (Bouvier, Cabot, Yon, & Grisch, 2020). The number density peak is related to incipient soot particles freshly produced at the boundary limit between the inner injection flow and the inner recirculation zone (IRZ). In this zone, ethylene fuel contained in the rich inner premixed flow is then thermally decomposed into polycyclic aromatic

hydrocarbons (PAH) that are known to be the precursors of soot particles. On the other hand, soot aggregates sampled along the burner axis are considered as mature soot particles. IRZ in swirled flames are known to produce stabilized areas where hot gases are trapped due to a pressure difference between its lower and upper extremities. The chemical composition in P1 to P3 conditions consists of burnt gases with radical species, but also PAH and soot aggregates. As the flow velocity is quite low and temperature of hot gases is quite high, various physico-chemical processes can occur and impact the soot particle growth or oxidation processes. At P1 condition, IRZ is predominantly composed of unburnt gases (i.e. PAHs) and soot aggregates. The large residence time induced by low velocities in this area enables the growth of soot particles by aggregation. In contrast, the increase of the swirl intensity in the P2 condition involves a stronger recirculation of burnt gases containing radical species such as OH towards the center of the flame. These radicals consume PAH's and unburnt molecules, which interrupts the particle surface growth. Soot aggregates also undergo oxidation, which can consume all of the smaller particles and partially consume the larger ones, and decrease their diameter. This trend is exacerbated in the P3 operating condition, where oxidation is so high that few soot particles are detected.

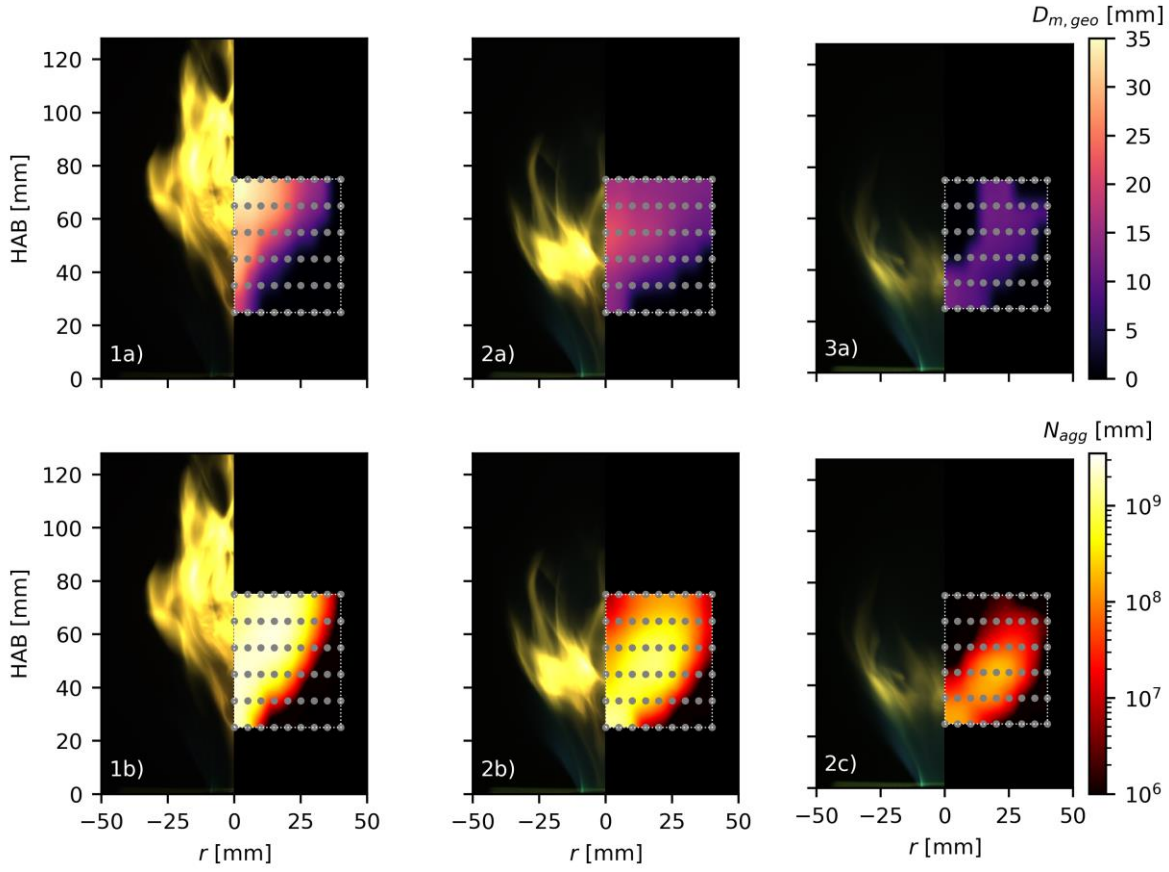

Fig. 4 Cartographies of a) median value of particle electrical mobility diameters and b) aggregate number concentrations measured by the SMPS on P1 (left), P2 (center) and P3 (right)

3. Soot size determination by angular scattering

The 2D angular scattering laser diagnostic offering the capability to perform measurements at high repetition rate has been specifically developed in the current study. As reminder, the intensity of the scattered light, resulting from the interaction of the laser beam with soot particles, varies with the scattering angle at which the light scattered is collected. Applied in the flame corresponding to the operating condition P1, the analysis of the scattering signal in function of the scattering angular variation provides opportunities to measure the soot gyration diameters D_g.

3.1 Principles of 2D-MALS

The vertical-vertical polarized light intensity from soot particles may be appropriately described by the Rayleigh-Debye-Gans theory for Fractal Aggregates (RDG-FA):

$$I_{vv}(\theta,\lambda) = I_0(\lambda) V_m N_{agg} \frac{x_p^6}{k^2} F(m) \frac{k_f^2}{D_p^{2D_f}} \int_0^{+\infty} D_g^{2D_f} f\left(qR_g\right) p\left(D_g\right) dD_g \tag{3}$$

In this expression, θ is the scattering angle, λ the incident laser wavelength, I_0 the incident laser irradiance, N_{agg} the number of aggregates contained in a measurement volume V_m. k is the wave vector, $x_p = 4\pi/D_p$ the size factor, and $F(m)$ the scattering function depending of the complex refractive index m. D_p is the primary particle diameter, D_f the fractal dimension, and the integral represents the sum of the contributions of each single aggregate. As illustrated in Eq. (3), the evaluation of soot aggregate sizes by elastic scattering is challenging because of the many unknown terms, like for instance the aggregate number concentration N_{agg} or the scattering coefficient $F(m)$. A method to circumvent this constraint consists in the collection of the scattered light intensity at two scattering angles (De Luliis, Cignoli, Benecchi, & Zizak, 1998). The ratio of both intensities, also called the dissymmetry ratio R_{vv}, eliminates the angle-independent terms.

$$\begin{aligned} R_{vv}\left(\theta,\theta_{ref}\right) &= \frac{I_{vv}(\theta)}{I_{vv}\left(\theta_{ref}\right)} \\ R_{vv}\left(\theta,\theta_{ref}\right) &= \frac{V_m(\theta)\int_0^{+\infty} D_g^{2D_f} f\left(q(\theta)R_g\right) p\left(D_g\right) dD_g}{V_m\left(\theta_{ref}\right)\int_0^{+\infty} D_g^{2D_f} f\left(q(\theta_{ref})R_g\right) p\left(D_g\right) dD_g} \end{aligned} \tag{4}$$

Assuming further properties on soot particles distributions, this equation can be numerically solved to determine a median gyration diameter $D_{g,geo}$: The parameter f represents the fractal nature of soot, modelled in our case by the RDG-FA theory. The probability density function $p\left(D_g\right)$ describes the polydispersity in size of the aggregate population. As observed in various studies, aggregate

populations in flames generally display a log-normal distribution. Thus, the probability density function $p(D_g)$ can be defined according to following expression:

$$\frac{dp(D_g)}{dD_g} = \frac{1}{D_g \ln \sigma_{g,geo} \sqrt{2\pi}} \exp\left[-\frac{1}{2}\left(\frac{\ln D_g - \ln D_{g,geo}}{\ln \sigma_{g,geo}}\right)^2\right] \quad (5)$$

The geometric standard deviation $\sigma_{g,geo}$ is assumed to be equal to 1.6, a value commonly found in the literature. Light intensity collected by the camera at 90° is interpreted as a soot aggregate number concentration thanks to time-averaged auto-compensating LII data performed in a previous study (Bouvier, Yon, Liu, Cabot, & Grisch, 2021).

2.3 Experimental set-up

The experimental set-up used for 2D angular scattering is depicted in fig. 5. The laser source is a high-speed pulsed Nd:YAG laser (Edgewave), with a repetition rate of 1 kHz and producing a wavelength of 532 nm. The laser pulse energy (~22 mJ) is controlled thanks to a half-wave plate and a Glan-Taylor polarizer. The laser beam is then transformed through a set of two cylindrical lenses (f= -20 mm and 500 mm) and a converging spherical one (f = 1 m), yielding a 120 µm wide and 50 mm laser sheet. To collect the light scattering of soot particles, three high-speed phantom V2012 cameras are used. They are equipped with 100 mm objectives (ZEISS Milvus 2/100M, f/2.0) and 532 nm dichroic filters (FWHM = 10 nm) to only collect the scattered elastic light. The cameras are positioned at scattering angles of $\theta_1 = 45°$, $\theta_2 = 90°$ and $\theta_3 = 135°$. Tilted cameras, used for the measurement of median aggregate gyration diameters, are equipped with Scheimpflug mounts to superimpose their focal plane with the laser sheet.

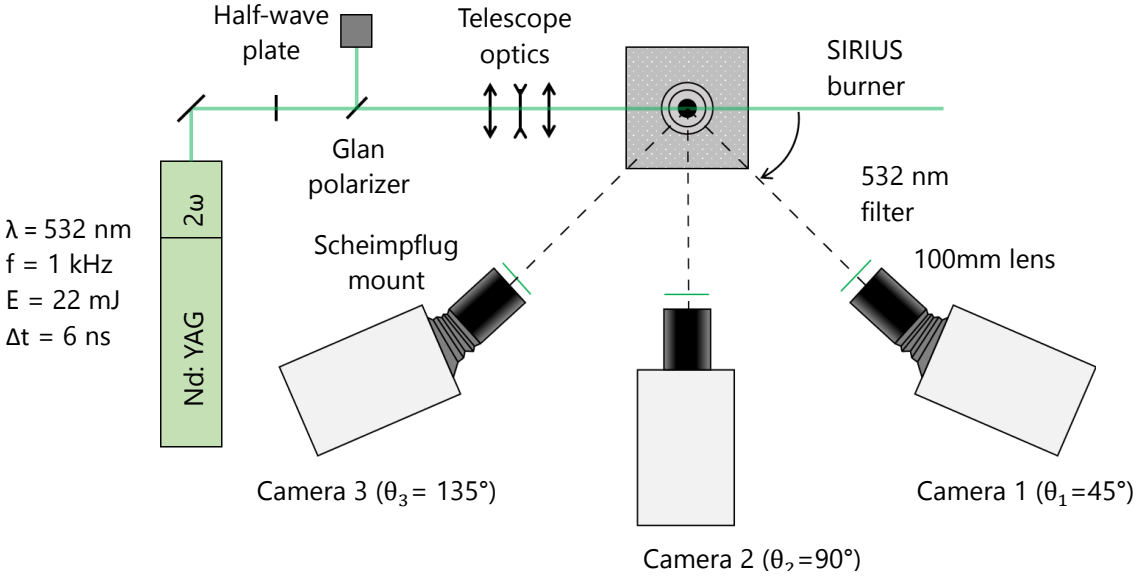

Fig. 5 Experimental apparatus for aggregate size measurement by angular scattering technique

4. Comparison between in-and ex-situ measurements

In a second step, the samples analyzed by SMPS are compared with soot size measurements performed by the 2D-MALS diagnostic. However, both techniques give experimental data on several scalar parameters which are not directly comparable. Indeed, a SMPS measurement gives access to an equivalent electric mobility diameter of each aggregate (D_m), and provides an average per size class, while the optical technique enables the measurement of the average gyration diameter (D_g) of soot particles contained in the probe volume, assuming some properties on soot population such as the size polydispersity.

4.1. Results pre-processing procedure

Samples analyzed by SMPS are compared with soot size measurements performed by the optical technique. Prior to compare results issued from both diagnostics, data have to be pre-processed. This task is performed in two parts. The first one is devoted to the diameter conversion while the second one is focused on the temporal averaging of high-speed optical measurements.

4.1.1 Conversion from electrical mobility diameter to gyration diameter

A conversion of the measured diameters by SMPS is required to enable a direct comparison between in- and ex-situ techniques. Indeed, the complex shape of the soot aggregates prevents any rigorous definition of the aggregate "size". However, this is counterbalanced by the use of equivalent diameters (usually that of a sphere), based on specific properties such as mass or volume, for example. The SMPS used in this study takes advantage of the notion of equivalent electric mobility diameter. For a non-spherical particle, the measured electric mobility diameter (D_m) corresponds to that of a sphere characterized by the same electric mobility, defined as follows [5]:

$$F_{drag} = \frac{3\eta D_m v_{drag}}{C_c(D_m)} \quad (6)$$

F_{drag} is the electrostatic force induced by the potential difference inside the column, v_{drag} the particle migration velocity, η the kinetic viscosity of the carrier gas and C_c the Cunningham slip correction factor. When entering into the SMPS device, soot aggregates are first charged by a radiation source, and then pass through the mobility diameter (DMA), where they are exposed to an electric field. The voltage difference induces a migration of charged particles, enabling their classification according to their electrical mobility. On the other side, the 2D-MALS laser diagnostic gives access to the average gyration diameter (D_g) of the aerosol contained in a probe volume V_m.

The diameter of gyration, D_g, is equivalent to the diameter of a sphere offering the same resistance to a change in angular velocity. For an aggregate constituted by monomers of same size, the radius of gyration is defined as the average root squared distance of monomers (with a radius R_p) from the aggregate center of mass.

$$R_g^2 = \frac{3}{5}R_p + \frac{1}{N_p}\sum_i r_i^2 \tag{7}$$

r_i is the distance between the i-th monomer and the aggregate center of mass. Unlike the electric mobility diameter, the gyration diameter is a purely geometric parameter, which does not depend on thermodynamic conditions, and is therefore generally preferred. To compare performances of both measurement techniques, a conversion process is exploited using the following semi-empirical model (Yon, Bescond, & Ouf, 2015),

$$\frac{\mathrm{D_g}}{D_m} = \frac{C_c(D_p)}{C_c(D_m)} k_f^{-1/D_f} N_p^{\frac{1}{D_f}(1-\Gamma)} \tag{8}$$

Γ is a Gaussian cumulative function determined experimentally, which only depends on the flow regime, represented by the Knudsen number of D_p:

$$\Gamma = 1.378\left[\frac{1}{2} + \frac{1}{2}\mathrm{erf}\left(\frac{K_n(D_p) + 4.4454}{10.628}\right)\right] \tag{9}$$

This model requires information on soot aggregate morphology, represented by the fractal parameters D_f and k_f. In our case, these parameters are fixed as for the angular scattering technique: 1.77 and 1.94.

4.1.1 Statistical data processing

Soot production generated by the flames issued from SIRIUS burner are highly intermittent. When a SMPS scans an aerosol during several tens of seconds, the measured aggregate size distribution is considered as stationary. On the contrary, the 2D-MALS diagnostic delivers single-shot measurements (i.e. few ns) and a statistical analysis of these measurements is therefore required in order to compare them with results obtained by the sampling probe technique. For every measurement position, a temporal averaging of 8000 instantaneous soot size measurements is performed and compared with the corresponding SMPS distribution, whom diameters have been previously converted into gyration diameters. For a pair of images i captured by the two high-speed cameras, a population of aggregates contained in a pixel of the camera at a given location

(HAB, r) is namely characterized by its particle number density N_{agg}, associated with its assumed log-normal shape distribution (Eq. (5)) of parameters $D_{g,geo}$ and $\sigma_{g,geo}$:

$$\begin{cases} \dfrac{dp(D_g)}{dD_g}(\mathrm{HAB}, r, i) = \dfrac{1}{D_g \ln \sigma_{g,geo} \sqrt{2\pi}} \exp\left[-\dfrac{1}{2}\left(\dfrac{\ln D_g - \ln D_{g,geo}(\mathrm{HAB}, r, i)}{\ln \sigma_{g,geo}}\right)^2\right] \\ N_{agg}(\mathrm{HAB}, r, i) \end{cases} \quad (10)$$

The temporal averaging of aggregate size distributions consists in an arithmetical weighted by the local aggregate number density:

$$\begin{cases} \overline{\dfrac{dp(D_g)}{dlnD_g}}(\mathrm{HAB}, r, i) = \dfrac{1}{N_{pix}\overline{N_{agg}}(\mathrm{HAB}, r, i)} \displaystyle\sum_{j=1}^{N_{pix}} N_{agg}(\mathrm{HAB}(j), r(j)) \dfrac{dp(D_g)}{dlnD_g}(\mathrm{HAB(j)}, r(j)) \\ \overline{N_{agg}}(\mathrm{HAB}, r, i) = \dfrac{1}{N_{pix}} \displaystyle\sum_{j=1}^{N_{pix}} N_{agg}(\mathrm{HAB}(j), r(j)) \end{cases} \quad (11)$$

4.2 Results and discussion

The data processing developed in section 4.1 has been applied to data recorded in the flames: The distributions of the electrical mobility diameters recorded by SMPS were converted into gyration diameters, and gyration diameters measured by the 2D-MALS diagnostic were time-averaged. Although the addition of log-normal distributions does not yield to a log-normal one, it could be observed that the averaged global distribution still follows a log-normal law. Then, the two resulting soot size distributions were fitted by a lognormal distribution to find their corresponding median gyration diameter. An example of a resulting comparison of measurements carried out along a flame radius at HAB = 55 mm is depicted in Fig. 6. A good similarity can be observed on gyration diameters, with mean values contained between 20 and 30 nm. Concerning the local particle number density, all measurements are of the same amount of order: between 1 and 3x10^9 aggregates per cm^3. Results acquired by the sampling probe are about 1.5 times larger than those obtained by the 2D-MALS diagnostic, suggesting that these differences may only originate from a systematic error due to the calibrations of the sampling probe and optical diagnostics. In a more general way, the contributions to measurement uncertainty, that have not been detailed in the present article, are manifold: One can mention, for the sampling probe technique, the sampling probe intrusiveness that disturbs the flame, but also the calibration of the sampling line, which could not be performed under similar operating conditions. Concerning the multi-angular

scattering measurements, the model used to associate light scattering with gyration diameters, the RDG-FA theory, assumes that aggregates are composed of uniform spherical primary particles. Assumptions made about aggregate morphology can significantly alter the predictions of the RDG-FA model and thus lead to biased results. Finally, despite the estimated uncertainties of the two techniques, the results are close to each other, giving a high degree of confidence in the validity of the soot aggregate sizes and concentrations measured in this type of turbulent flames.

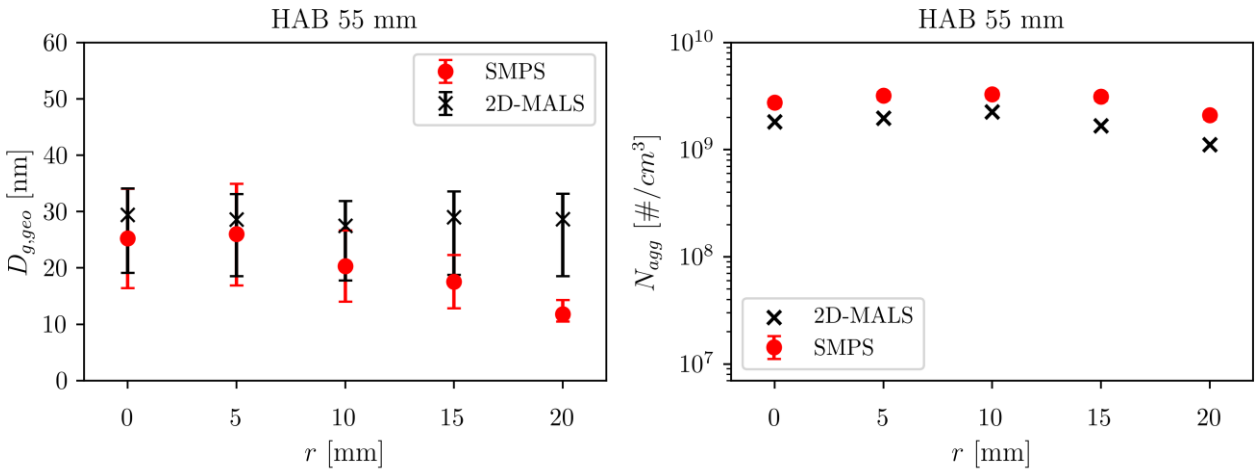

Fig. 6: Comparison between soot size distributions obtained by angular scattering and SMPS measurements, with P1 at HAB = 55 mm

5. Conclusion

The measurement of the size and number density of soot particles were conducted in stratified swirled premixed ethylene-air flames at atmospheric pressure. For this purpose, a classical approach was used, consisting in sampling soot particles inside the flame, analyzing them with a Scanning Mobility Particle Sizer, and finally measuring their electrical mobility diameters. In a second step, measurements made by the sampling probe technique were compared with those carried out with an innovative high-speed optical technique, called 2D-MALS, where the scattering angular dependence of the light scattering by the soot aggregates enables to measure the gyration diameters. A direct comparison of the results obtained with both measurement diagnostics is not feasible, especially because the basic principles of these measurement techniques are very different from each other. To overcome this constraint, a methodology for post-processing the measured scaler parameters was developed. First, the electrical mobility diameters recorded by the Scanning Mobility Particle Sizer were converted into gyration diameters using a semi-empirical model from the literature. Then, a time average of the gyration diameters obtained by the angular scattering technique was performed, considering that the SMPS measurements performed at each flame

position over a relatively large acquisition time converge to a single value. Finally, direct comparisons were performed at a height above the burner outlet of 55 mm. The good similarity between the results provides a remarkably high degree of confidence in the quality of the measurements for both measurement systems investigated. Furthermore, the results suggest that a comparison of soot aggregate size and number density measurements between a sampling probe and a light scattering technique is still possible in turbulent flames at atmospheric pressure. While the current work has focused on the performances of SMPS and the 2D-MALS approach on a one-to-one basis, future work will also address the application of these diagnostics to high-pressure two-phase flames for which measurements are made in confined environments.

References

Bouvier, M., Cabot, G., Yon, J., & Grisch, F. (2020). On the use of PIV, LII, PAH-PLIF and OH-PLIF for the study of soot formation and flame structure in a swirl stratified premixed ethylene/air flame. *Proceedings of the Combustion Institute, 38*(1), 1851-1858.

Bouvier, M., Yon, J., Liu, F., Cabot, G., & Grisch, F. (2021). Application of planar auto-compensating laser-induced incandescence to low-sooting turbulent flames and investigation of the detection gate width effect. *Aerosol Science and Technology*.

De Luliis, S., Cignoli, F., Benecchi, S., & Zizak, G. (1998). Determination of soot parameters by a two-angle scattering–extinction technique in an ethylene diffusion flame. *Applied Optics, 37*.

DeCarlo, P., Slowik, J. G., Worsnop, D. R., Davidovits, P., & L., J. J. (n.d.). Particle Morphology and Density Characterization by Combined Mobility and Aerodynamic Diameter Measurements. Part 1: Theory. *Aerosol Science and Technolog, 38*(112).

Giechaskiel, B., Carriero, M., Martini, G., Krasenbrink, A., & Scheder, D. (2009). Calibration and Validation of Various Commercial Particle NumberMeasurement Systems. *SAE International Journal of Fuels and Lubricants*.

ICAO. (2016). *Trends in Emissions that affect Climate Change.*

Kulkarni, P., Baron, P. A., & Willelke, K. (2011). *Aerosol Measurement. Principles, Techniques and Applications.* John Wiley & Sons.

Mulla, I., Yon, J., Lefèvre, G., Lecordier, B., & Honoré, D. (2017). Determination of soot volume fraction and particle size distribution in turbulent non- premixed butane and ethylene jet flames through LII, PPS and SMPS measurements. *European Combustion Meeting*.

Ramanathan, V., & Carmichael, G. (2008). Global and regional climate changes due to black carbon. *Nature Geosciences*, 221-227.

Yon, J., Bescond, A., & Ouf, F.-X. (2015). A simple semi-empirical model for effective density measurements of fractal aggregates. *Journal of Aerosol Science*, 28-37.